Letter

Discovery of a Novel cGAMP Competitive Ligand of the Inactive Form of STING

Tony Siu, Michael D Altman, Gretchen A Baltus, Matthew Childers, J Michael Ellis, Hakan Gunaydin, Harold Hatch, Thu Ho, James Jewell, Brian M Lacey, Charles A Lesburg, Bo-Sheng Pan, Berengere Sauvagnat, Gottfried K Schroeder, and Serena Xu

ACS Med. Chem. Lett., **Just Accepted Manuscript** • DOI: 10.1021/acsmedchemlett.8b00466 • Publication Date (Web): 06 Dec 2018

Discovery of a Novel cGAMP Competitive Ligand of the Inactive Form of STING

Tony Siu,[*,†] Michael D. Altman,[§] Gretchen A. Baltus,[‡] Matthew Childers,[†] J. Michael Ellis,[†] Hakan Gunaydin,[§] Harold Hatch,[⊥] Thu Ho,[¥] James Jewell,[†] Brian M. Lacey,[⊥] Charles A. Lesburg,[∞] Bo-Sheng Pan,[⊥] Berengere Sauvagnat,[⊥] Gottfried K. Schroeder,[⊥] and Serena Xu[⊥]

[†]Departments of Chemistry, [‡]Immunology, [§]Chemistry Modeling and Informatics, [⊥]In Vitro Pharmacology, [¥]Target Protein Design and [∞]Structural Chemistry, Merck & Co., Inc., 33 Avenue Louis Pasteur, Boston, MA 02115

KEYWORDS: STING, active site dimers, ligand-ligand interactions, permeability, inflammatory disease, druggability.

ABSTRACT: Drugging large protein pockets is a challenge due to the need for higher molecular weight ligands which generally possess undesirable physicochemical properties. In this communication, we highlight a strategy leveraging small molecule active site dimers to inhibit the STING protein, which contains a large symmetric binding pocket. By taking advantage of the 2:1 binding stoichiometry, maximal buried interaction with STING protein can be achieved while maintaining the ligand physicochemical properties necessary for oral exposure. This mode of binding requires unique considerations for potency optimization including simultaneous optimization of protein-ligand as well as ligand-ligand interactions. Successful implementation of this strategy led to the identification of **18**, which exhibits good oral exposure, slow binding kinetics, and functional inhibition of STING mediated cytokine release.

The activation of the innate immune system through nucleic acid sensing is a key mechanism of host defense from viruses and bacteria.[1-2] Recent discoveries in the cyclic GMP-AMP synthase–stimulator of interferon genes (cGAS-STING) pathway have captured the attention of the pharmaceutical industry due to the pathway's role in host pathogen defense, immuno-oncology and autoimmune diseases.[3] Upon activation by double stranded DNA (dsDNA), cGAS synthesizes the cyclic dinucleotide secondary messenger 2',3'-cyclic GMP-AMP (cGAMP) which then activates the endoplasmic reticulum (ER)–membrane adaptor protein STING.[4-5] Activated STING initiates a cascade that ultimately primes the immune system to restrict viral spread through the activation and production of type 1 interferons (IFN) and pro-inflammatory cytokines such as tumor necrosis factor-α (TNF-α).

While stimulation of STING and the production of type 1 interferons is an important mechanism for pathogen defense and tumor control, failure to regulate chronic inflammatory signaling can lead to autoimmunity.[6] The mis-localization of nuclear and mitochondrial dsDNA in the cytoplasm combined with the inability of cGAS to differentiate foreign from self dsDNA is a potential trigger for type 1 interferon production and auto-inflammation.[7-9] Type 1 interferon and mis-localized dsDNA are hallmarks and key drivers for the pathogenesis of autoimmune diseases such as systemic lupus erythematosus (SLE).[10] Additionally, loss of function mutations in the DNA exonuclease TREX1 lead to the excessive type 1 interferon signature found in Aicardi–Goutières syndrome (AGS) and SLE, implicating the role of self dsDNA in auto-inflammation.[11] Furthermore, monogenic Mendelian diseases with STING gain of function mutations such as familial chilblain lupus (FCL) support the role of STING in autoimmune disease.[12] These studies collectively suggest that inhibition of STING might regulate DNA-driven inflammatory diseases.

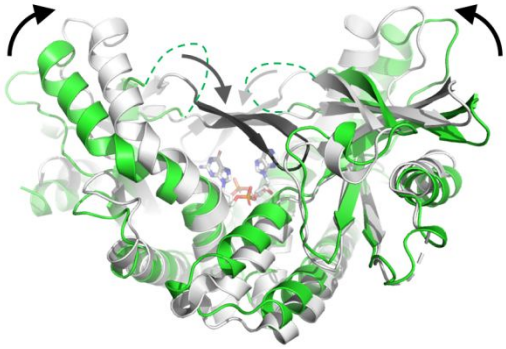

Figure 1: Conformational comparison of STING apoprotein ("open" conformation, green, PDB 6MXo) with a STING:cGAMP complex ("closed", white, from PDB 4KSY). Residues which become ordered upon cGAMP binding are shown as dark gray β-strands in the closed conformation and green dashes in the open

conformation. cGAMP is shown as sticks in the center of the STING homodimer. Arrows indicate the direction of movement of the central α-2 helix upon cGAMP binding and the ordering of the central β-sheet.

Although the biological rationale linking STING to inflammatory diseases supports the development of a STING antagonist, the general lack of biochemical mechanistic understanding of STING activation combined with the absence of known small molecule tools suggested that identification of binders to the STING protein might pose a significant challenge.[13-14] Based on biophysical and X-ray crystallographic data, the STING C-terminal domain (referred to as STING henceforth) exists as a symmetrical dimer with the ligand binding site located at the interface between the two monomers, which has been shown to be the binding site of the natural agonist cGAMP and the mouse-specific agonist DMXAA.[15] Comparison of the structures of STING apoprotein with cGAMP-bound protein highlights two distinct conformations (**Figure 1**). The STING apoprotein adopts an "open" conformation, with residues 226 to 241 in each monomer. In contrast, STING complexed with an agonist adopts a "closed" conformation wherein, the central α-2 helix from each monomer (approximately residues 171 to 185) tilt toward each other by roughly 15° and residues 226 to 241 in each monomer, disordered in the "open" conformation, adopt a four-stranded β-sheet. These distinct conformational states suggest that the stabilization of the "open" conformation might lead to inactivation whereas stabilization of the "closed" conformation might lead to activation of the protein. [15-17]

With the knowledge of the ligand binding site, a druggability assessment was performed on the apoprotein to probe the feasibility of discovering a suitable ligand which might preferentially bind to the "open" conformation.[18] The total protein solvent accessible surface area (SASA) is calculated to be 390 Å^2, which would require a ligand of ~700 Da to occupy.[19] Of the total SASA, 60% is polar SASA which limits maximal binding affinity driven by hydrophobic interactions. Finally, the calculated volume of the ligand binding site is 952 Å^3, suggesting the possibility for binding a large complex ligand. Unfortunately, physicochemical properties of ligands of this nature are not generally consistent with orally bioavailable drug-like small molecules.[20] Another complexity in targeting the STING protein is the requirement for a small molecule antagonist to be competitive with the high molecular weight, high affinity endogenous ligand, cGAMP. Together, these considerations highlight the challenges for identifying small molecule STING antagonists with the appropriate properties necessary for oral exposure.

The large ligand binding surfaces and volumes calculated for STING necessitated a unique approach. Our investigation was inspired by the recognition that two molecules of the mouse-specific STING agonist DMXAA are bound to a single STING homodimer (**Figure 2**).[15] This 2:1 binding ratio is possible due to the C2 symmetry of the STING protein which allows each DMXAA molecule to interact with a single STING monomer. Our strategy to maximize binding efficiency was to exploit the intrinsic symmetry of the STING protein by identifying small molecules that can bind to the "open" conformation in a 2:1 ratio to the STING homodimer. Such a binding stoichiometry could afford fuller occupation of the large binding site, and thus effectively compete with cGAMP, while still maintaining physiochemical properties compatible with oral drugs.

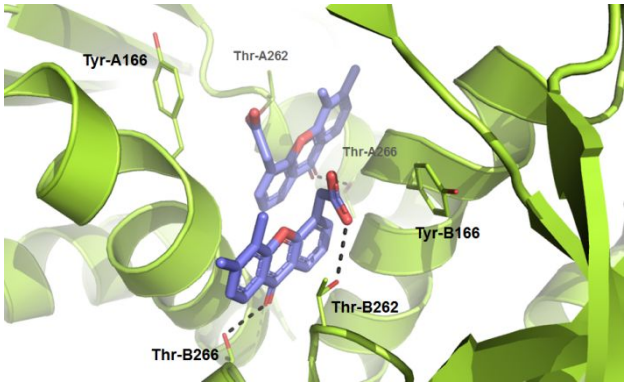

Figure 2: X-ray structure of DMXAA molecules bound to mouse STING in the "closed" conformation (PDB 4LOL).[15] STING protein is colored green, and DMXAA is shown in blue sticks. Intermolecular interactions between DMXAA and Thr-262 and Thr-266 are indicated by black dashes. There is also a salt bridge between the DMXAA carboxylate group and Arg-237 (not shown; corresponds to Arg-238 in human STING).

Table 1: Profile of screening hit compound 1.

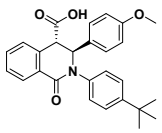

	1 (*rac*)
HAQ STING IC_{50} (nM)[a]	7,300
MW	430
cLogP	6.21
LBE/ LLE[b]	0.22/1.4

[a]Values in this table are determined by the HAQ STING cGAMP displacement assay and are the means from at least n = 2 experiments. [b]Values are calculated from pIC50 – ALogP98

Encouraged by the possibility of utilizing 2:1 binding stochiometry to offset the challenge of a large binding pocket, we turned to our Automated Ligand

Identification System (ALIS), which has emerged as a robust platform for hit identification.[21] Compound **1** was initially identified as a low activity hit (IC_{50} = 7,300 nM).

Crystallographic studies confirmed 2:1 binding. Not only do two molecules of **1** complement each other's shape and bind to one dimer of STING, but they also bind to the "open" conformation (**Figure 3**) suggesting these molecules might function as an antagonist. Two interlocking copies of the compound are bound in the central cleft of the STING homodimer, and the absolute configuration is unambiguously assigned as (*S*, *S*).

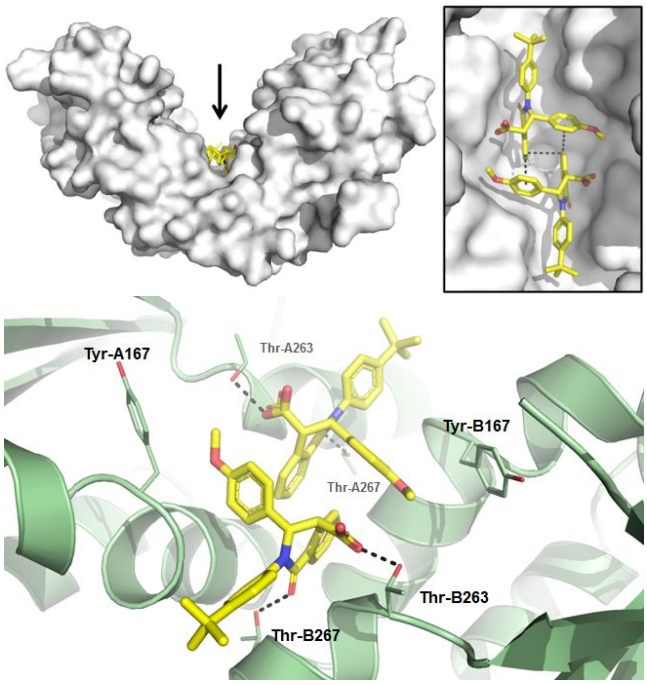

Figure 3: X-ray structure of **1** in STING protein showing 2:1 binding and ligand interactions (PDB 6MX3). **Top:** STING is shown as a white surface, with **1** colored yellow. The inset shows a close-up view of the two copies of **1** from the direction indicated by the arrow. **Bottom:** close-up of polar interactions between **1** and side chains of Thr-263 and Thr-267 of both STING chains. Sidechain atoms of Tyr-167 are also shown as sticks. Dashed lines indicate selected van der Waals interactions and hydrogen bonds.

Compound **1** makes predominantly hydrophobic interactions, punctuated by several polar contacts. The carboxylate group forms a hydrogen bond with the side chain of Thr-263 and the exocyclic oxygen forms a hydrogen bond with the side chain of Thr-267. The methoxyphenyl group maintains van der Waals contact with the protein, and the *para-tert*-butyl group projects towards open solvent. There are a number of disordered residues which have been omitted from the crystallographic model, including many which become ordered upon agonist binding. In addition, there are various interactions between the two molecules of **1** found in the ligand binding site. The aromatic ring of the isoquinolone not only engages in face-to-face π-stacking with the aromatic ring of the other copy of **1**, but also engages in edge-to-face π-stacking with the methoxyphenyl group.[22] This network of interlocking π-stacking interactions between the two copies of the molecules reinforces binding to the STING protein and is likely the source of observed cooperative binding (*vida infra*). The two monomers form a substantial dimer interface within the active site, burying approximately 274 Å^2 of water accessible surface area, emphasizing the importance of ligand-ligand interactions in the observed binding mode. [23]

Scheme 1: Synthesis of tetrahydroisoquinolone analogs

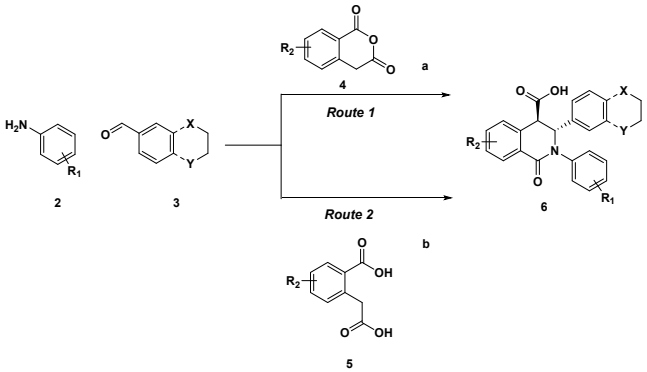

a) $InCl_3$, Cs_2CO_3, MeCN, microwave 100 °C, 2-38% ; b) toluene, reflux, 31-81%.

An advantage of the tetrahydroisoquinolone series is the flexibility of the synthesis which allows for rapid diversity generation in a one-pot synthesis. From the initial hit, SAR was generated using the procedures highlighted in **Scheme 1**. In this initial approach, aniline (**2**), homopthalic anhydride (**4**), and benzaldehyde (**3**) were heated in a microwave reactor with cesium carbonate (Cs_2CO_3) and indium chloride ($InCl_3$) as a catalyst. However, the yields were poor and the purification was complicated by mixtures of side products. By switching to the diacid (**5**) and removing $InCl_3$, reactions proceeded more cleanly to desired products.

Despite a clear view of the compound-protein interactions, early SAR highlighted the challenge of designing molecules with improved affinity. **Table 2** lists a few examples to illustrate initial struggles to improve potency. While computational studies supported the replacement of the methoxyphenyl with various substitutions, these modifications did not lead to improvements in activity with the exception of the benzodioxane compound **7**. Because these compounds are bound to STING as dimers, special consideration is required to rationalize the observed SAR. In addition to stabilizing the protein-ligand complex relative to the

unbound state, the interaction between the bound monomers must also be considered. To this end, we redesigned our computational models to include an evaluation of dimer association energy using density functional theory (DFT) to estimate active site ligand-ligand complementarity in addition to docking studies to model protein-ligand interactions.[24]

Table 2: Initial representative SAR on tetrahydroisoquinoline screening hit

Compound	Structure	IC_{50} (nM)[a]
7 (rac)	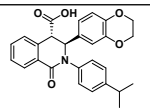	2700
8 (rac)	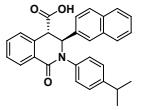	>20000
9 (rac)	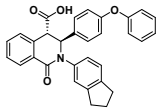	>20000
10 (rac)	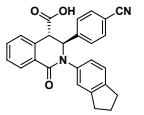	>20000
11 (rac)	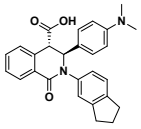	>20000
12 (rac)	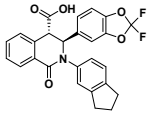	>20000

[a]Values in this table are determined by the HAQ STING cGAMP displacement assay and are the means from at least n = 2 experiments.

Consistent with previous observations regarding substituent effects on edge-to-face aromatic interactions, the predicted dimer association energies track with the electron richness of the accepting ring as well as steric interaction/repulsion across the dimer interface (see SI).[25] For example, the electron-rich benzodioxyl **7** has a more favorable predicted dimer association energy which may, in part, explain its improved binding activity, while naphthyl **8** and *p*-cyanophenyl **10**, being more electron poor, are expected to exhibit less self-interaction which may contribute to their weaker STING binding. Difluorobenzodioxole **12** is predicted to have a steric clash across the dimer interface where fluorine on one monomer is in close proximity to the carboxylate group of the other monomer.

Encouraged by these calculations, efforts were made to simultaneously design subtle variations of the aryl ring to enhance both ligand-ligand and protein-ligand interactions. Toward that end, various heteroatoms were incorporated to increase the ligand π interactions. In order to compare the analogs as matched pairs, the compounds were synthesized as single enantiomers with the more potent chloro *t*-butyl phenyl solvent piece (**Table 3**). Although none of these analogs were dramatically differentiated from compound **13**, the experimental results were consistent with our hypothesis that activity was dependent on both ligand and protein interactions when compared to **Table 2**.

Table 3: Benzodioxane variants

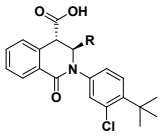

Compound	R	IC_{50} (nM)[a]
13	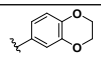	84
14		384
15		41
16		670
17		106

[a]Values in this table are determined by the HAQ STING cGAMP displacement assay and are the means from at least n = 2 experiments.

Although **13** exhibited potent activity in the cell-free ligand displacement assay, it displayed low oral bioavailability (%F = 5) which may be a consequence of the modest permeability (MDCK Papp = 9 x 10^{-6} cm/s).[26] We postulated that an increased ionization of **13** negatively impacted the passive permeability. The pK_a is calculated to be 3.4, lower than the typical value (pK_a = 4-5) for an aliphatic carboxylic acid, likely due to an inductive effect from the aromatic isoquinolone core. Accordingly, extension of the carboxylic acid to the homologated acid (compound **18**) preserved activity and increased the calculated pK_a to 4.3. To rule out any unexpected conformational change induced by **18**, crystallographic studies were conducted (**Figure 4**). As with **1**, 2 molecules of extended acid **18** bind a single STING homodimer in the "open" conformation. The extended acid group and the lone pair of the isoquinonlone amide maintain the same interactions with Thr-263 and Thr-267, which are found in the identical conformation as in the complex with **1**. Unique to this structure is the benzodioxane stacking with Tyr-167. The aromatic fluorine fills a pocket created by Gly-158 and Leu-159 at the bottom of the central binding groove, while

the aromatic chlorine further fills the pocket created by Ile-165 and Ala-270.

Consistent with our hypothesis, the increase in calculated pK_a translated to a combination of improved permeability (Papp = 18 x 10^{-6} cm/s) as well as improved oral bioavailability (%F = 60; solubility and Cl_{int} remains constant allowing for the interpretation that permeability is the main driver for improvement, **Table 4**). Overall, the pharmacokinetics properties for compound **18** are modest with high intrinsic clearance. Kinetic binding assessment of **13** and **18** by surface plasmon resonance (Biacore) revealed a slow k_{off} (**13**, $t_{1/2}$ = 35 min; **18**, $t_{1/2}$ = 62 min). Moreover, consistent with cooperative binding, data fitting required a two-step model (Figure S1A-C and supporting information). These observations may reflect an overall increase in stability when a second molecule binds to STING.

Table 4: *In vitro* profile of lead STING ligands

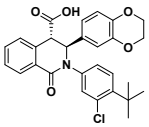

13

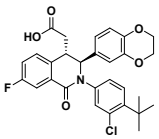

18

	13	**18**
HAQ STING IC_{50} (nM)[a]	84	68
LBE/LLE[b]	0.28/2.87	0.27/2.58
pKa[c]	3.4	4.3
MDCK Papp (x 10^{-6} cm/s)[26]	9	18
%F	5	60
FASSIF (uM) pH(6.5)	151	187
Hep Cl_{int}(r/h)(mL/min/kg)[d]	158/28	240/31
Rat Cl_p (mL/min/kg)[e]	38	45
SPR $t_{1/2}$ (min)[d]	35	62
THP1 Cell IC50 (nM)[f]	11500	11000
THP1 Cell EC50 (nM)[d]	>30000	>30000

[a]Values in this table are determined by the HAQ STING cGAMP displacement assay and are the means from at least n = 2 experiments. [b]Values are calculated from pIC50 – ALogP98. [c]Values calculated from ACD LABS 11.0. [d]See supporting information. [e]Dose; rat iv 0.5 mpk as a solution in PEG400:H_2O (60:40 (v/v)), po: 1 mpk as a solution in PEG400:H_2O (60:40 (v/v)). [f]Values in this table are determined by inhibiting IFNβ production in cGAMP stimulated THP1 cells and are the means from at least n = 2 experiments.

Although we have identified molecules that are able to displace cGAMP and stabilize the "open" conformation of STING, a key assumption is that stabilizing the "open" conformation will prevent all STING signaling. To test this hypothesis, THP1 cells were incubated with **13** and **18** with and without cGAMP stimulation. The compounds did not stimulate IFNβ production (**13** EC50= >30,000 nM; **18** EC50=>30000 nM; **Table 4**), but modestly inhibited cGAMP-induced IFNβ production (**13** IC50 = 11,500 nM; **18** IC50 = 11,000 nM; **Table 4**), with a >100-fold shift in potency from binding to the functional cell assay. Our observations are consistent with these compounds functioning as STING antagonists. Considering that the assay is stimulated with nonphysiological levels of cGAMP, the cellular IC50 may not be an accurate representation of antagonist potency.[27]

In conclusion, we have identified weak antagonists of STING-mediated signaling that binds to the cGAMP binding site in the inactive "open" conformation. By exploiting the natural symmetry of the STING protein and utilizing 2:1 binding stoichiometry, these compounds are able to fully occupy the binding pocket while mitigating the undesirable physicochemical properties associated with larger ligands. As a consequence of the 2:1 binding ratio, two dimensional optimization of the protein-ligand and ligand-ligand interactions was necessary to improve potency. This approach led to the discovery of compound **18** with slow dissociation kinetics, good oral bioavailability, and ability to inhibit cGAMP dependent signaling *in vitro*.

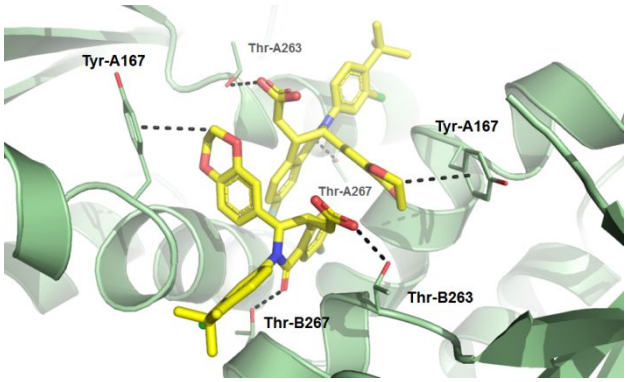

Figure 4: Co-crystal structure of **18** bound to STING protein (PDB 6MXE) showing interactions with Thr-263 and Thr-267, with sidechain atoms depicted as sticks. As observed with **1**, the compound binds in a 2:1 ratio to the STING homodimer and makes the same interactions, with additional van der Waals contact with the sidechain phenol of Tyr-167. The homologated carboxylate group maintains a hydrogen bond interaction with Thr-263.

Supporting Information. Synthetic procedures and analytical data of selected compounds, conditions for all biological assays, and X-ray crystallographic methods and statistics, DFT methods, Surface Plasmon Resonance and protein preparation, off-target profile. This material is available free of charge on the internet at http://pubs.acs.org.

Acknowledgements. We thank J. Presland for helpful discussions and P. Schwartz for assistance with developing the kinetic model for Biacore fitting.

Accession Codes : STING apoprotein: 6MX0; STING complex with **1**: 6MX3; STING complex with **18**: 6MXE.

Corresponding Author

*Phone: 617-992-2386. E-mail: tony_siu@merck.com

References

1. Ahlers, L. R.; Goodman, A. G., Nucleic acid sensing and innate immunity: signaling pathways controlling viral pathogenesis and autoimmunity. *Curr Clin Microbiol Rep* **2016,** *3* (3), 132-141.
2. Wu, J.; Chen, Z. J., Innate immune sensing and signaling of cytosolic nucleic acids. *Annu Rev Immunol* **2014,** *32*, 461-88.
3. Junt, T.; Barchet, W., Translating nucleic acid-sensing pathways into therapies. *Nat Rev Immunol* **2015,** *15* (9), 529-44.
4. Sun, L.; Wu, J.; Du, F.; Chen, X.; Chen, Z. J., Cyclic GMP-AMP synthase is a cytosolic DNA sensor that activates the type I interferon pathway. *Science* **2013,** *339* (6121), 786-91.
5. Chen, Q.; Sun, L.; Chen, Z. J., Regulation and function of the cGAS-STING pathway of cytosolic DNA sensing. *Nat Immunol* **2016,** *17* (10), 1142-9.
6. Ahn, J.; Barber, G. N., Self-DNA, STING-dependent signaling and the origins of autoinflammatory disease. *Curr Opin Immunol* **2014,** *31*, 121-6.
7. Ahn, J.; Gutman, D.; Saijo, S.; Barber, G. N., STING manifests self DNA-dependent inflammatory disease. *Proc Natl Acad Sci U S A* **2012,** *109* (47), 19386-91.
8. Ahn, J.; Ruiz, P.; Barber, G. N., Intrinsic self-DNA triggers inflammatory disease dependent on STING. *J Immunol* **2014,** *193* (9), 4634-42.
9. Gao, D.; Li, T.; Li, X. D.; Chen, X.; Li, Q. Z.; Wight-Carter, M.; Chen, Z. J., Activation of cyclic GMP-AMP synthase by self-DNA causes autoimmune diseases. *Proc Natl Acad Sci U S A* **2015,** *112* (42), E5699-705.
10. Rumore, P. M.; Steinman, C. R., Endogenous circulating DNA in systemic lupus erythematosus. Occurrence as multimeric complexes bound to histone. *J Clin Invest* **1990,** *86* (1), 69-74.
11. Rice, G. I.; Rodero, M. P.; Crow, Y. J., Human disease phenotypes associated with mutations in TREX1. *J Clin Immunol* **2015,** *35* (3), 235-43.
12. Konig, N.; Fiehn, C.; Wolf, C.; Schuster, M.; Cura Costa, E.; Tungler, V.; Alvarez, H. A.; Chara, O.; Engel, K.; Goldbach-Mansky, R.; Gunther, C.; Lee-Kirsch, M. A., Familial chilblain lupus due to a gain-of-function mutation in STING. *Ann Rheum Dis* **2017,** *76* (2), 468-472.
13. Koch, P. D.; Miller, H. R.; Yu, G.; Tallarico, J. A.; Sorger, P. K.; Wang, Y.; Feng, Y.; Thomas, J. R.; Ross, N. T.; Mitchison, T., A High Content Screen in Macrophages Identifies Small Molecule Modulators of STING-IRF3 and NFkB Signaling. *ACS Chem Biol* **2018,** *13* (4), 1066-1081.
14. Haag, S. M.; Gulen, M. F.; Reymond, L.; Gibelin, A.; Abrami, L.; Decout, A.; Heymann, M.; van der Goot, F. G.; Turcatti, G.; Behrendt, R.; Ablasser, A., Targeting STING with covalent small-molecule inhibitors. *Nature* **2018,** *559* (7713), 269-273.
15. Gao, P.; Ascano, M.; Zillinger, T.; Wang, W.; Dai, P.; Serganov, A. A.; Gaffney, B. L.; Shuman, S.; Jones, R. A.; Deng, L.; Hartmann, G.; Barchet, W.; Tuschl, T.; Patel, D. J., Structure-function analysis of STING activation by c[G(2',5')pA(3',5')p] and targeting by antiviral DMXAA. *Cell* **2013,** *154* (4), 748-62.
16. Zhang, X.; Shi, H.; Wu, J.; Zhang, X.; Sun, L.; Chen, C.; Chen, Z. J., Cyclic GMP-AMP containing mixed phosphodiester linkages is an endogenous high-affinity ligand for STING. *Mol Cell* **2013,** *51* (2), 226-35.
17. Ramanjulu, J. M.; Pesiridis, G. S.; Yang, J.; Concha, N.; Singhaus, R.; Zhang, S. Y.; Tran, J. L.; Moore, P.; Lehmann, S.; Eberl, H. C.; Muelbaier, M.; Schneck, J. L.; Clemens, J.; Adam, M.; Mehlmann, J.; Romano, J.; Morales, A.; Kang, J.; Leister, L.; Graybill, T. L.; Charnley, A. K.; Ye, G.; Nevins, N.; Behnia, K.; Wolf, A. I.; Kasparcova, V.; Nurse, K.; Wang, L.; Li, Y.; Klein, M.; Hopson, C. B.; Guss, J.; Bantscheff, M.; Bergamini, G.; Reilly, M. A.; Lian, Y.; Duffy, K. J.; Adams, J.; Foley, K. P.; Gough, P. J.; Marquis, R. W.; Smothers, J.; Hoos, A.; Bertin, J., Design of amidobenzimidazole STING receptor agonists with systemic activity. *Nature* **2018**.
18. Le Guilloux, V.; Schmidtke, P.; Tuffery, P., Fpocket: an open source platform for ligand pocket detection. *BMC Bioinformatics* **2009,** *10*, 168.
19. Cheng, A. C.; Coleman, R. G.; Smyth, K. T.; Cao, Q.; Soulard, P.; Caffrey, D. R.; Salzberg, A. C.; Huang, E. S., Structure-based maximal affinity model predicts small-molecule druggability. *Nat Biotechnol* **2007,** *25* (1), 71-5.
20. Lipinski, C. A.; Lombardo, F.; Dominy, B. W.; Feeney, P. J., Experimental and computational approaches to estimate solubility and permeability in drug discovery and development settings. *Adv Drug Deliv Rev* **2001,** *46* (1-3), 3-26.
21. Annis, D. A.; Nickbarg, E.; Yang, X.; Ziebell, M. R.; Whitehurst, C. E., Affinity selection-mass spectrometry screening techniques for small molecule drug discovery. *Curr Opin Chem Biol* **2007,** *11* (5), 518-26.
22. Meyer, E. A.; Castellano, R. K.; Diederich, F., Interactions with aromatic rings in chemical and biological recognition. *Angew Chem Int Ed Engl* **2003,** *42* (11), 1210-50.
23. Buried accessible surface area was calculated using MOE by taking the difference in accessible surface area between the dimer and two monomers. Molecular Operating Environment (MOE), 2013.08; Chemical Computing Group ULC, 1010 Sherbooke St. West, Suite #910, Montreal, QC, Canada, H3A 2R7, 2018.
24. See supplementary section for methods and free energy calculations of analogs tested
25. Sinnokrot, M. O.; Sherrill, C. D., Substituent effects in pi-pi interactions: sandwich and T-shaped configurations. *J Am Chem Soc* **2004,** *126* (24), 7690-7.
26. Irvine, J. D.; Takahashi, L.; Lockhart, K.; Cheong, J.; Tolan, J. W.; Selick, H. E.; Grove, J. R., MDCK (Madin-Darby canine kidney) cells: A tool for membrane permeability screening. *J Pharm Sci* **1999,** *88* (1), 28-33.
27. Cell viability has been accounted for in the THP1 assay; for list of off target hits for 13 see supporting information

For Table of Content Use Only

Discovery of a Novel cGAMP Competitive Ligand of the Inactive Form of STING

Tony Siu,[*,†] Michael D. Altman,[§] Gretchen A. Baltus,[‡] Matthew Childers,[†] J. Michael Ellis,[†] Hakan Gunaydin,[§] Harold Hatch,[⊥] Thu Ho,[¥] James Jewell,[†] Brian M. Lacey,[⊥] Charles A. Lesburg,[∞] Bo-Sheng Pan,[⊥] Berengere Sauvagnat,[⊥] Gottfried K. Schroeder,[⊥] and Serena Xu[⊥]

[†]Departments of Chemistry, [‡]Immunology, [§]Chemistry Modeling and Informatics, [⊥]In Vitro Pharmacology, [¥]Target Protein Design and [∞]Structural Chemistry, Merck & Co., Inc., 33 Avenue Louis Pasteur, Boston, MA 02115